Available online at www.sciencedirect.com
SCIENCE DIRECT®
International Journal of Heat and Mass Transfer 48 (2005) 1716–1726
International Journal of HEAT and MASS TRANSFER
www.elsevier.com/locate/ijhmt

# Fluid flow and mass transfer modelling in lysozyme ultrafiltration

Vítor Magueijo [a], Viriato Semião [b], Maria Norberta de Pinho [a,*]

[a] Department of Chemical Engineering, Torre Sul, Instituto Superior Técnico, Av. Rovisco Pais, 1049-001 Lisbon, Portugal
[b] Department of Mechanical Engineering, Instituto Superior Técnico, Av. Rovisco Pais, 1049-001 Lisbon, Portugal

Received 13 June 2004; received in revised form 24 November 2004
Available online 20 January 2005

**Abstract**

This work addresses the mass transfer modelling of ternary solutions, water/lysozyme/sodium chloride, in the slit feed channel of a ultrafiltration (UF) cell. Permeation experiments are performed using a laboratory-made UF cellulose acetate membrane, characterised by an hydraulic permeability of $2.05 \times 10^{-11}$ m/s/Pa and a molecular weight cut-off of 30 kDa. The simulation of the UF operating conditions with recourse to computer fluid dynamics allows the prediction of the selective permeation performance in terms of permeation fluxes and concentration polarization. The predictions of the permeation fluxes based on different mass transport assumptions are compared with experimental ones and a good agreement is obtained.


*Keywords:* Concentration polarization; Modelling; Ultrafiltration; Cross diffusion; Protein

## 1. Introduction

### 1.1. Preamble

Ultrafiltration (UF) is a membrane pressure driven process with industrial importance in the purification and concentration of macromolecular solutions, namely protein solutions. The present work addresses the transport phenomena, momentum and mass transfer, associated to lysozyme ultrafiltration. Lysozyme is a globular protein and an enzyme that can be easily found in nature, as for example in egg white and human tears. Hen's egg white lysozyme is a natural preservative with antibacterial action that has been widely used in refrigerated prepared foods. It is very stable and due to its lytic activity, selectively destroys certain harmful microorganisms allowing beneficial bacteria in food to survive. It is a comprehensively studied enzyme, with many applications in food and pharmaceutical industry, and commonly used as a research model protein.

In UF, a pressurized feed flows tangentially to a permeable membrane that acts as a selective barrier (Fig. 1), rejecting partially or totally the solute(s) and permeating the solvent that usually is water. The rejection of the solute(s) is associated to an increase of the solute(s) concentration(s) at the membrane surface and to the appearance of a phenomenon known as concentration polarization (CP). This phenomenon affects the process performance by causing membrane fouling and by

* Corresponding author. Tel.: +351 218 417 488; fax: +351 218 499 242.
*E-mail address:* marianpinho@ist.utl.pt (M.N. de Pinho).

0017-9310/$ - see front matter © 2005 Elsevier Ltd. All rights reserved.
doi:10.1016/j.ijheatmasstransfer.2004.11.009

**Nomenclature**

| | |
|---|---|
| $B_{LL}$ | second virial osmotic coefficient for lysozyme, mol · m$^3$/kg$^2$ |
| $C$ | solute concentration, mol/m$^3$ |
| CP | concentration polarization |
| $D_A$ | mass diffusion coefficient of solute A, m$^2$/s |
| $f_A$ | apparent rejection coefficient for solute A, $f_A = 1 - (\omega_{Ap}/\omega_{A0})$ |
| $h$ | channel height, m |
| $J$ | solute molecular flux, m/s |
| $k$ | transport coefficient in the film model, m |
| $l$ | channel length, m |
| $L_p$ | hydraulic permeability, m/s/Pa |
| $M_L$ | protein (lysozyme) molecular weight, kg/mol |
| MWCO | molecular weight cut-off |
| $p$ | pressure, Pa |
| $\Re$ | ideal gas constant (=8.315 J/K/mol) |
| $Re$ | circulation Reynolds number, $Re = u_0 \cdot h/v$ |
| $S_\phi$ | source term in the transport equation of property $\phi$ |
| $Sc$ | Schmidt number, $Sc = \mu/(\rho \cdot D)$ |
| $T$ | temperature, K or °C |
| TOC | total organic carbon |
| $u$ | velocity component in the $x$-direction, m/s |
| $u_0$ | uniform velocity at the channel entrance (feed), m/s |
| $v$ | velocity component in the $y$-direction, m/s |
| $v_p$ | permeation velocity/flux, m/s |
| $x, y$ | spatial coordinates, m |

*Greek symbols*

| | |
|---|---|
| $\delta$ | film thickness, m |
| $\Delta P$ | transmembrane pressure, Pa |
| $\Delta\Pi$ | total transmembrane osmotic pressure, Pa |
| $\Delta\Pi_A$ | transmembrane osmotic pressure of solute A, Pa |
| $\phi$ | generic property |
| $\Gamma_A$ | concentration polarization coefficient for solute A, $\Gamma_A = (\omega_{Am}/\omega_{A0}) - 1$ |
| $\Gamma_\phi$ | diffusion coefficient of generic property $\phi$, kg/m/s |
| $\lambda_D$ | Debye length, nm |
| $\mu$ | fluid viscosity, Pa s |
| $v$ | fluid kinematic viscosity, m$^2$/s |
| $\Pi_A$ | osmotic pressure of solute A, Pa |
| $\rho$ | fluid density, kg/m$^3$ |
| $\omega_A$ | mass fraction of solute $A$, kg$_A$/kg$_{solution}$ |

*Subscripts*

| | |
|---|---|
| 0 | channel inlet, feed |
| m | membrane/fluid interface |
| p | permeate |
| L | lysozyme |
| S | salt (NaCl) |

decreasing the permeation flux (productivity). Consequently, in the design and optimisation of UF membrane modules, concentration polarization must be quantitatively analysed in order to minimize its effects. Concentration polarization is essentially a mass transfer problem that is highly dependent on the feed flow structure, and therefore the coupling of mass transfer and hydrodynamics will be given special attention in the present work.

### 1.2. Mass transfer in membrane processes

The first and more common approach for the quantification of the CP in ultrafiltration has been through the use of the film model that sets its grounds in two basic assumptions:

(a) the mass transport resistance is essentially located in a thin film layer of constant thickness, $\delta$, adjacent to the membrane/fluid interface;
(b) in the film layer the mass transport occurs essentially by diffusion (Fick's law).

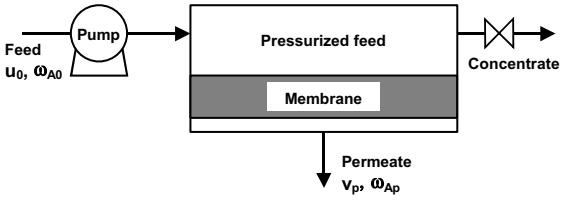


Fig. 1. Schematics of tangential ultrafiltration.

A differential mass balance in this film layer leads to a solute transport equation that is integrated across $\delta$ and yields

$$J = -\frac{D_{AB}}{\delta}\ln\left(\frac{C_{Am} - C_{Ap}}{C_{A0} - C_{Ap}}\right) = -k \cdot \ln\left(\frac{C_{Am} - C_{Ap}}{C_{A0} - C_{Ap}}\right) \quad (1)$$

where $J$ is the permeate flux; $D_{AB}$ is the solute mass diffusion coefficient; $C_{Am}$, $C_{A0}$ and $C_{Ap}$ are the solute concentrations at the membrane surface, in the feed bulk solution and in the permeate, respectively, and $k$ is the mass transport coefficient given by $k = D_{AB}/\delta$.

The two above-mentioned very restrictive assumptions make of the film model a very simplified description of reality and led many authors like Probstein et al. [1] and Zydney [2] to an extensive discussion in the literature about its associated inaccuracy. The key parameter of the film model, the film thickness, is extremely difficult to quantify. In order to overcome this difficulty, empirical mass transfer correlations have been used to predict the mass transport coefficient ($k$). Two types of correlations are usually used to predict $k$: correlations based in analogies between momentum, heat and mass transfer and correlations from experimental mass transfer data. However, both types of correlations pertain to impermeable solid/fluid interfaces that are very different from the membrane/feed flow interfaces where membrane permeation highly influences the mechanisms of mass transfer and the development of concentration polarization. Situations of high permeation rates and of complex feed flow structures with recirculation zones, render the film model particularly inadequate.

Brian [3] presented one of the first attempts of modelling simultaneously the hydrodynamic and mass transfer phenomena in a reverse osmosis (RO) flat membrane module. A two-dimensional flow was assumed and the resort to a finite difference numerical approach allowed the prediction of the salt concentration polarization in RO. Sherwood et al. [4] presented an analytical infinite series solution for the CP of salt in reverse osmosis. These authors could already anticipate that the development of more permeable membranes would bring about the importance of the high permeation rates on the CP phenomena. Geraldes et al. [5–7], making recourse to computer fluid dynamics (CFD) have investigated flow and mass transfer in nanofiltration where the permeation rates are situated between the ones of RO and UF. Lebrun et al. [8] and Bouchard et al. [9], used CFD for the study of flow and mass transfer phenomena in UF and predicted the concentration polarization in slits with laminar flow. Rosén and Trägårdh [10] have presented predictions for UF in tubular membrane modules.

The literature above discussed addresses the modelling of binary solutions. In the present work aqueous solutions containing a protein and a salt are ternary systems, and to model effectively the UF of such systems, an accurate description of the multicomponent nature of the mass transport is required. In fact, protein diffusion can be enhanced or hindered by the concentration gradient of the salt itself, and vice-versa. Also, in UF, due to the concentration polarization phenomenon, the species being rejected by the membrane develop transversal concentration profiles at the membrane vicinity that need an accurate local description. The association of that with multicomponent diffusion may play an important role in the overall mass transport. In this work, the very complex situation of multicomponent mass transfer occurring in the UF of the ternary system water/lysozyme/sodium chloride, is modelled and simulated with recourse to the most adequate tool, which is computer fluid dynamics. The predictions under different mass transfer conditions are compared with experimental data.

## 2. Mathematical model

The geometry of the system defined in this work and used in the numerical simulations is illustrated in Fig. 2.

The mathematical model used in the simulations of the UF of an aqueous ternary solution containing lysozyme and NaCl as solutes, is described below. Model equations are set for the momentum and mass transport phenomena occurring in the fluid phase and fluid/membrane interface. The model assumptions are: (a) steady state, two-dimensional, incompressible and isothermal laminar flow in the feed channel; (b) the fluid and solute properties (density, viscosity and mass diffusion coefficients) vary with the salt concentration; (c) existence of cross diffusion, i.e., the salt diffuses due to its concentration gradient and also due to the protein concentration gradient (and vice-versa); (d) the permeation velocity, $v_p$, depends on the transmembrane osmotic pressure with protein and salt contributions taken into account and (e) the mass fractions of the solutes in the permeate are known and kept equal to the experimental value, along the entire channel length.

For the defined geometric system (Fig. 2) and under the above-referred conditions, the momentum and solute transport equations for the ternary solution, water/protein/salt, without reaction are the following:

(1) Global continuity equation

$$\frac{\partial(\rho u)}{\partial x}+\frac{\partial(\rho v)}{\partial y}=0 \tag{2}$$

(2) Momentum equation in the $x$-direction

$$\begin{aligned}&\frac{\partial(\rho uu)}{\partial x}+\frac{\partial(\rho vu)}{\partial y}\\&\quad=-\frac{\partial p}{\partial x}+\left[\frac{\partial}{\partial x}\left(\mu\frac{\partial u}{\partial x}\right)+\frac{\partial}{\partial y}\left(\mu\frac{\partial u}{\partial y}\right)\right]\\&\qquad+\left(\frac{\partial}{\partial x}\mu\frac{\partial u}{\partial x}+\frac{\partial}{\partial y}\mu\frac{\partial v}{\partial x}\right)-\frac{2}{3}\frac{\partial}{\partial x}\mu\left(\frac{\partial u}{\partial x}+\frac{\partial v}{\partial y}\right)\end{aligned} \tag{3}$$

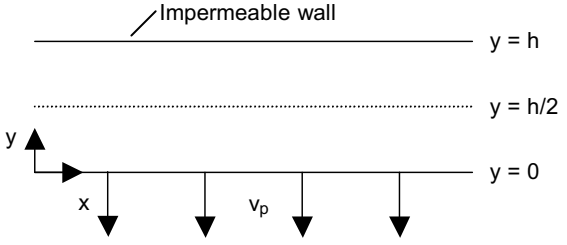


Fig. 2. Geometry used for the numerical simulations.

(3) Momentum equation in the $y$-direction

$$\frac{\partial(\rho uv)}{\partial x}+\frac{\partial(\rho vv)}{\partial y} = -\frac{\partial p}{\partial y}+\left[\frac{\partial}{\partial x}\left(\mu\frac{\partial v}{\partial x}\right)+\frac{\partial}{\partial y}\left(\mu\frac{\partial v}{\partial y}\right)\right] + \left(\frac{\partial}{\partial x}\mu\frac{\partial u}{\partial y}+\frac{\partial}{\partial y}\mu\frac{\partial v}{\partial y}\right)-\frac{2}{3}\frac{\partial}{\partial y}\mu\left(\frac{\partial u}{\partial x}+\frac{\partial v}{\partial y}\right) \tag{4}$$

(4) Protein (lysozyme) continuity equation

$$\frac{\partial(\rho u\omega_{\mathrm{L}})}{\partial x}+\frac{\partial(\rho v\omega_{\mathrm{L}})}{\partial y} = \frac{\partial}{\partial x}\left(\rho D_{\mathrm{LL}}\frac{\partial\omega_{\mathrm{L}}}{\partial x}\right)+\frac{\partial}{\partial y}\left(\rho D_{\mathrm{LL}}\frac{\partial\omega_{\mathrm{L}}}{\partial y}\right) + \frac{\partial}{\partial x}\left(\rho D_{\mathrm{LS}}\frac{\partial\omega_{\mathrm{S}}}{\partial x}\right)+\frac{\partial}{\partial y}\left(\rho D_{\mathrm{LS}}\frac{\partial\omega_{\mathrm{S}}}{\partial y}\right) \tag{5}$$

(5) Salt (NaCl) continuity equation

$$\frac{\partial(\rho u\omega_{\mathrm{S}})}{\partial x}+\frac{\partial(\rho v\omega_{\mathrm{S}})}{\partial y} = \frac{\partial}{\partial x}\left(\rho D_{\mathrm{SS}}\frac{\partial\omega_{\mathrm{S}}}{\partial x}\right)+\frac{\partial}{\partial y}\left(\rho D_{\mathrm{SS}}\frac{\partial\omega_{\mathrm{S}}}{\partial y}\right) + \frac{\partial}{\partial x}\left(\rho D_{\mathrm{SL}}\frac{\partial\omega_{\mathrm{L}}}{\partial x}\right)+\frac{\partial}{\partial y}\left(\rho D_{\mathrm{SL}}\frac{\partial\omega_{\mathrm{L}}}{\partial y}\right) \tag{6}$$

In Eqs. (2)–(6), $\rho$ is the fluid density; $\mu$ is the fluid viscosity; $\omega_{\mathrm{L}}$ and $\omega_{\mathrm{S}}$ are the mass fractions of protein and salt, respectively; $D_{\mathrm{LL}}$, $D_{\mathrm{SS}}$, $D_{\mathrm{LS}}$ and $D_{\mathrm{SL}}$ are the mass diffusion coefficients (main terms and cross terms) for the ternary system water–protein–salt. In this work, one has used the ternary diffusion coefficients obtained by Albright et al. [11] and Annunziata et al. [12] for the system water–lysozyme–sodium chloride. These authors have studied this system intensively and extracted a significant amount of experimental thermodynamic data. Eqs. (2)–(6) are solved together with the following boundary conditions of the studied system:

(1) Channel inlet ($x = 0$): plug flow profiles—velocity and mass fractions;

$$\forall y: \quad u = u_0,\ v = 0,\ \omega_{\mathrm{L}} = \omega_{\mathrm{L0}},\ \omega_{\mathrm{S}} = \omega_{\mathrm{S0}} \tag{7}$$

(2) Channel outlet ($x = l$): fully developed flow and negligible axial diffusion;

$$\forall y: \quad \frac{\partial u}{\partial x}=0,\ \frac{\partial v}{\partial x}=0,\ \frac{\partial\omega_{\mathrm{L}}}{\partial x}=0,\ \frac{\partial\omega_{\mathrm{S}}}{\partial x}=0 \tag{8}$$

(3) Impermeable wall: top wall ($y = h$);

$$\forall x: \quad u = 0,\ v = 0,\ \frac{\partial\omega_{\mathrm{L}}}{\partial y}=0,\ \frac{\partial\omega_{\mathrm{S}}}{\partial y}=0 \tag{9}$$

(4) Permeable wall/membrane: bottom wall ($y = 0$);

a. Flux continuity at the fluid/membrane interface

$$\forall x: \quad u = 0,\ \ v = -v_{\mathrm{p}} = -L_{\mathrm{p}}(\Delta P - \Delta\Pi) \tag{10}$$

b. Solute flux continuity at the fluid/membrane interface

i. Protein

$$\forall x: \quad D_{\mathrm{LL}}\frac{\partial\omega_{\mathrm{L}}}{\partial y}+D_{\mathrm{LS}}\frac{\partial\omega_{\mathrm{S}}}{\partial y}=v_{\mathrm{p}}(\omega_{\mathrm{Lm}}-\omega_{\mathrm{Lp}}) \tag{11a}$$

ii. Salt

$$\forall x: \quad D_{\mathrm{SS}}\frac{\partial\omega_{\mathrm{S}}}{\partial y}+D_{\mathrm{SL}}\frac{\partial\omega_{\mathrm{L}}}{\partial y}=v_{\mathrm{p}}(\omega_{\mathrm{Sm}}-\omega_{\mathrm{Sp}}) \tag{11b}$$

In Eq. (10), $L_{\mathrm{p}}$ is the hydraulic permeability of the membrane, $\Delta P$ is the applied transmembrane pressure and $\Delta\Pi$ is the total transmembrane osmotic pressure. In Eq. (11a) and (11b), $\omega_{\mathrm{Lp}}$ and $\omega_{\mathrm{Sp}}$ are the mass fractions in the permeate of protein and salt, respectively; while $\omega_{\mathrm{Lm}}$ and $\omega_{\mathrm{Sm}}$ are respectively, the mass fractions of protein and salt at the membrane surface.

In order to obtain $v_{\mathrm{p}}$ using Eq. (10), first it is necessary to compute the value of $\Delta\Pi$. The total transmembrane osmotic pressure is a function of the mass fractions of the solutes in the permeate and at the membrane/fluid interface, i.e., $\Delta\Pi = f(\omega_{\mathrm{Lm}}, \omega_{\mathrm{Sm}}, \omega_{\mathrm{Lp}}, \omega_{\mathrm{Sp}})$. Nevertheless, the model assumes that the mass fractions of the solutes in the permeate are known values, hence $\Delta\Pi$ only depends on the unknown mass fractions of the solutes at the membrane/fluid interface: $\omega_{\mathrm{Lm}}$ and $\omega_{\mathrm{Sm}}$. Eqs. (10), (11a) and (11b) are solved by the following iterative procedure: first, the permeation flux, $v_{\mathrm{p}}$, is calculated through Eq. (10) using values of $\omega_{\mathrm{Lm}}$ and $\omega_{\mathrm{Sm}}$ from the previous iteration, then the obtained value of $v_{\mathrm{p}}$ is used in Eq. (11a) and (11b) in order to obtain the new/updated values of $\omega_{\mathrm{Lm}}$ and $\omega_{\mathrm{Sm}}$. The iterative procedure stops when the momentum and mass balances are satisfied.

## 3. Numerical procedure

The set of differential equations is integrated through the use of the finite volume formulation, and the governing equations—momentum equations and total mass plus solutes mass conservation equations—together with the appropriate boundary conditions are solved simultaneously. Eqs. (2)–(6) can be written in the general form of a generic differential transport equation

$$\frac{\partial(\rho u\phi)}{\partial x}+\frac{\partial(\rho v\phi)}{\partial y}-\frac{\partial}{\partial x}\left(\Gamma_{\phi}\frac{\partial\phi}{\partial x}\right)-\frac{\partial}{\partial y}\left(\Gamma_{\phi}\frac{\partial\phi}{\partial y}\right)-S_{\phi}=0 \tag{12}$$

Eq. (12) is the transport equation for a generic property $\phi$, containing a convection, a diffusion and source term ($S_{\phi}$), where $\Gamma_{\phi}$ is the diffusion coefficient of $\phi$. Equations having the form of Eq. (12) can be discretized. The transport equations (Eqs. (2)–(6)) are

discretized using the hybrid scheme. However, in the control volumes adjacent to the membrane surface, the protein and salt mass fluxes equations were discretized using the one-dimensional exact exponential solution. This procedure and the numerical implementation of the boundary conditions is extensively described by Patankar [13]. The SIMPLE algorithm is used to solve the problem of pressure–velocity coupling and to solve the pressure-correction equation (Patankar, [13]). After discretization, Eqs. (2)–(6) have an algebraic form and can be solved using a line-by-line Gauss–Seidel iteration method (Tri Diagonal Matrix Algorithm). The finite volume formulation was applied using a staggered grid strategy. A calculation grid with $50 \times 50$ nodes in both $x$ and $y$ directions was used. The grid was more refined near the channel inlet in the $x$-direction and more refined near the membrane surface in the $y$-direction. These are the regions where the velocities gradients (channel inlet) and mass fraction gradients (membrane surface) are more pronounced.

## 4. Experimental section

### 4.1. Materials

A cellulose acetate membrane (CA-I-1) was laboratory made by the phase inversion method described by Kunst and Sourirajan [14]. Table 1 lists the composition of the casting solution used in the preparation of the membrane.

This one, prior to the set-up in the permeation cell, was kept in a 0.5% $NaHSO_3$ solution under refrigeration.

The ternary solutions, water/protein/salt, were prepared with lysozyme (Chloride, grade VI from chicken egg white, lot 018H7019, MW 14500, 89% pure) from Sigma and sodium chloride (pro analysis from Merck). All the solutions were prepared with deionised water (specific conductivity $<5\ \mu S\,cm^{-1}$ at 25 °C). The pH of the prepared solutions ranged from 5.4 to 7.1.

### 4.2. Experimental set-up

The experimental set-up includes a permeation cell with a slit feed channel (Fig. 3). The permeation cell has two detachable parts. The upper part is a high-pressure chamber provided with a v-shaped inlet and outlet openings for optimal flow distribution of the feed. The lower part is the membrane stand and is provided with outlet openings for the withdrawal of the membrane permeate solution. The wet cellulose acetate membrane is mounted on a stainless steel porous plate embedded in this lower part of the cell, in such way that the active layer of the asymmetric membrane faces the feed solution on the pressurised side of the cell.

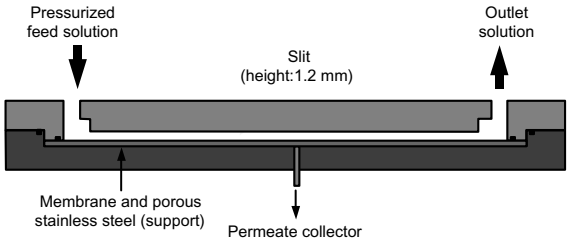


Fig. 3. Permeation cell with narrow rectangular channel.

Table 1
Composition of the casting solution

| Membrane CA-I-1 | % (w/w) |
|---|---|
| Cellulose Acetate 398 ( Eastman Kodak) | 13.95 |
| Acetone (p.a., Merck) | 79.07 |
| Magnesium perchlorate (p.a., Merck) | 3.49 |
| Deionised water | 3.49 |

The channel for the circulation of the pressurized feed, the cell upper part, is a slit with the channel height, $h$, very small compared to the other dimensions, length, $l$, and width, $w$. The geometrical characteristics support the consideration of a two-dimensional feed flow. This channel is analogous to the feed channel of the spiral wound membrane modules.

### 4.3. Procedure

#### 4.3.1. Characterization of the membrane

The membrane was first compacted for 2.5 h with recirculating water at an operating pressure ($\Delta P$) of $10 \times 10^5$ Pa and at a temperature of 25 °C. The membrane hydraulic permeability was determined through the slope of the straight line describing the variation of the pure water permeate fluxes versus the operating pressures, $\Delta P$, of 2, 4, 6 and $8 \times 10^5$ Pa. The water circulation Reynolds number, $Re$, was 1000.

To characterize the membrane in terms of molecular weight cut-off (MWCO), permeation experiments with reference solutes (PEGs synthesis grade from Merck and Dextrans from Pharmacia) were performed at 2 bar, $T = 25 \pm 0.5$ °C, and feed concentration of approximately 0.6 kg/m$^3$ ($Re = 1085$).

#### 4.3.2. Permeation of ternary aqueous solutions of lysozyme and NaCl

Solutions of lysozyme (0.3 kg/m$^3$) containing different NaCl concentrations were ultrafiltrated through membrane CA-I-1. For these ternary solutions, two Schmidt numbers are defined: one for the protein—$Sc_L = \mu/(\rho \cdot D_{LL})$, and another for the salt—$Sc_S = \mu/(\rho \cdot D_{SS})$. In the feed solutions, the $Sc_L$ varies from

6900 to 7900 and the $Sc_S$ varies from 610 to 630. The permeation experiments were carried out with a tangential circulation velocity, $u_0$, of 0.46 m/s ($Re$ = 615), and a temperature of 25 ± 0.25 °C. The operating conditions of applied pressure and temperature of the system were automatically controlled with the support of a Labtech® data acquisition and process control software. Experimental values of the permeate fluxes were measured within the pressure range: $2 \times 10^5$–$8 \times 10^5$ Pa and samples of feed and permeate were taken for analysis. At each applied pressure, permeation fluxes were measured after a stabilization time of at least 10 min. Feed pressure was measured with a precision of 0.01 bar and feed temperature with a precision of 0.01 °C.

The protein concentration was determined through the Lowry method described in Peterson [15]. The pH and the specific conductivity were measured with a Crison micro pH 2002 and a Crison conductimeter 525, respectively. The concentrations of reference solutes used in the membrane characterization were determined by a Dohrmann TOC analyser model DC-85A. The measurements of protein and reference solutes concentrations were all performed in triplicate.

## 5. Experimental results

### 5.1. Membrane characterisation

The hydraulic permeability ($L_p$) of the membrane is determined by plotting the experimental permeation fluxes for pure water ($v_{pw}$) versus the applied transmembrane pressure (Fig. 4) and fitting a straight line (Eq. (13)). The slope of the fitted line is the value of $L_p$ obtained directly from experimental data. The value of $L_p$ for membrane CA-I-1 is $2.1 \times 10^{-11}$ m/s/Pa.

$$v_{pw} = L_p \cdot \Delta P \tag{13}$$

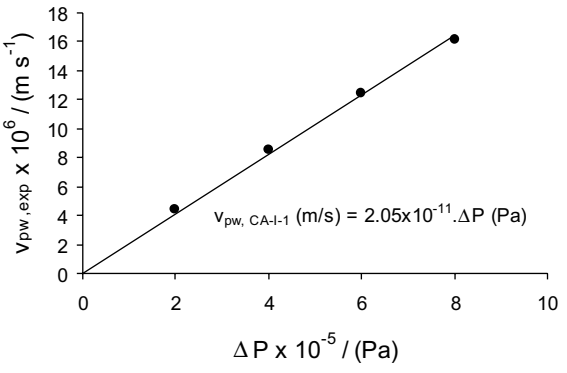


Fig. 4. Pure water permeation fluxes for membrane CA-I-1.

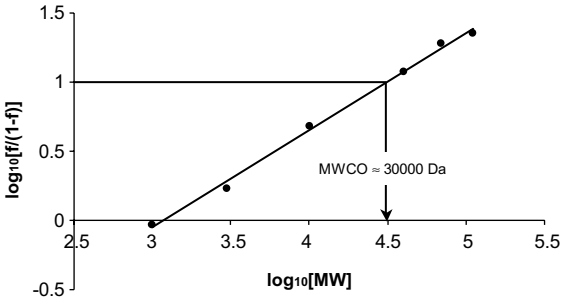


Fig. 5. Determination of the MWCO for membrane CA-I-1.

From permeation experiments, the apparent rejection coefficients ($f$) for reference solutes (PEGs and Dextrans) of increasing molecular weight (MW) were obtained. For a certain solute A, the apparent rejection coefficient, $f_A$, is defined as: $f_A = 1 - (\omega_{Ap}/\omega_{A0})$. Using the values of the apparent rejection coefficients for the reference solutes, the values of $\log_{10}[f/(1-f)]$ are plotted versus the values of $\log_{10}$[MW] (Fig. 5). Defining MWCO as the molecular weight of the solute being rejected at 90.9% ($f$ = 0.909), one can see that for $\log_{10}$[MWCO] corresponds $\log_{10}[f/(1-f)] = 1$. As shown in Fig. 5, a MWCO of approximately 30 kDa is obtained for the membrane CA-I-1.

### 5.2. Ultrafiltration of water/lysozyme/NaCl solutions

The experimental ultrafiltration results for solutions with a lysozyme concentration of 0.3 kg/m$^3$ and different NaCl concentrations of 0.001, 0.01, 0.1 and 0.5 M are shown in Fig. 6. In Fig. 6(a) the curves of the variation of the permeate fluxes with pressure are displaying lower values at increasing values of NaCl concentration. At higher pressures the deviation of these curves from the pure water fluxes is more pronounced. The Fig. 6(b) and (c) display respectively the variation with pressure of the rejection coefficients to lysozyme, $f_L$, and to NaCl, $f_S$, for solutions with increasing concentrations of sodium chloride. The membrane CA-I-1 strongly rejects the protein lysozyme while the NaCl is weakly rejected. More precisely, the values of $f_L$ are always higher than 92% and the values of $f_S$ always lower than 25%. The increase of NaCl concentration produces a decrease on the protein rejection, specially at lower pressures. There are three distinct curves, one for the solution without addition of NaCl, other for the NaCl concentration of 0.001 M and another for the NaCl concentrations of 0.01, 0.1 and 0.5 M. Fig. 6(c) shows that when the NaCl concentration in solution increases, the NaCl rejection coefficients decrease. The NaCl rejection coefficients vary linearly with pressure upon three distinct lines, one for the solution with NaCl concentration of 0.001 M, other for the NaCl concentrations of 0.01

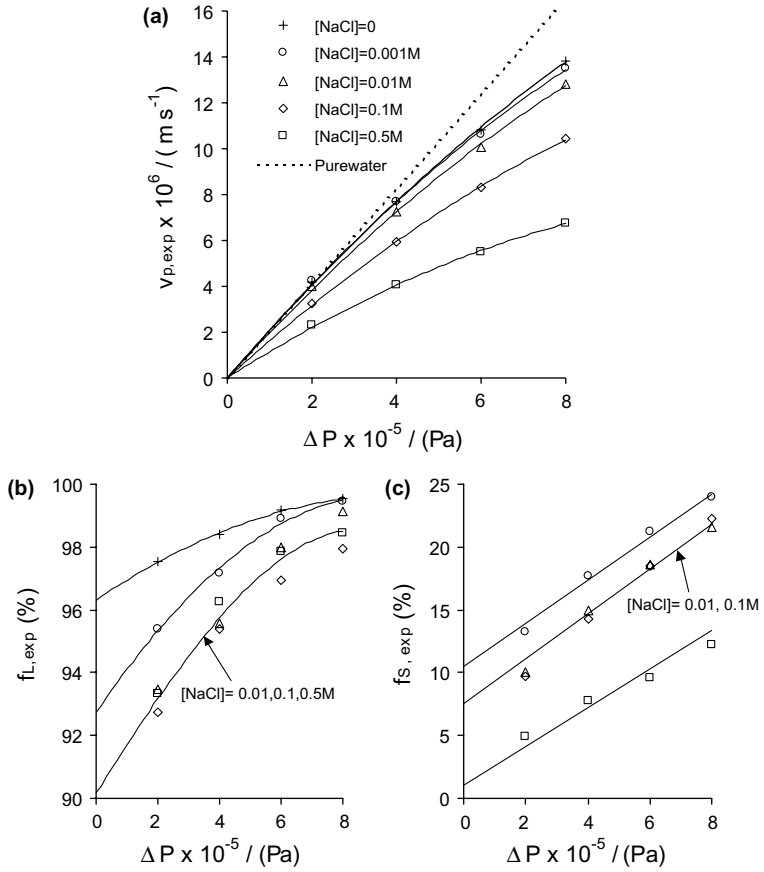


Fig. 6. Experimental results for the UF of water/lysozyme/NaCl solutions using membrane CA-I-1 ($u_0 = 0.46$ m/s, $T = 25 \pm 0.25$ °C): (a) Permeation fluxes; (b) apparent rejection coefficient for lysozyme, $f_L$; (c) apparent rejection coefficient for NaCl, $f_S$.

and 0.1 M and another for the NaCl concentration of 0.5 M. One should point out that the commercial lysozyme used in the preparation of the solutions is a product 89% pure, containing 11% in weight of stabilizing monovalent salts (sodium chloride and sodium acetate). All the prepared solutions have a concentration of commercial lysozyme ranging from 0.3 to 0.35 kg/m$^3$, hence, according to the product specifications and considering the NaCl as the only stabilizing salt present, the molar concentration of salt in a solution of lysozyme without addition of NaCl, ranges from $5.7 \times 10^{-4}$ to $6.6 \times 10^{-4}$ M.

## 6. CFD simulations

In this work, three different sets of simulations were performed to describe the UF of a solution containing water, lysozyme and NaCl under different mass transfer assumptions. They will be designated as simulations sets I, II and III.

*Set I*—Due to the fact that the membrane has an high MWCO (30 kDa), the NaCl rejection coefficients are very low and therefore one could expect that there is no significant salt accumulation adjacent to the membrane and the salt concentration polarization can be neglected. Based on that assumption, the NaCl continuity equation (Eq. (6)) and the corresponding boundary condition (Eq. (11b)) are not considered. Cross diffusion is also not taken into consideration and the cross diffusion terms in Eqs. (5) and (11a) are then neglected. Taking into consideration these assumptions, the Eqs. (2)–(5) are solved with the boundary conditions described in Eqs. (7)–(10), (11a). In Eq. (10), $\Delta\Pi$ is given by the following equation:

$$\Delta\Pi = \Delta\Pi_{\mathrm{L}} + \Delta\Pi_{\mathrm{S}} = (\Pi_{\mathrm{Lm}} - \Pi_{\mathrm{Lp}}) + (\Pi_{\mathrm{S0}} - \Pi_{\mathrm{Sp}}) \quad (14)$$

The Eq. (14) is an expression for the total osmotic pressure difference between both sides of the membrane (feed and permeate sides). The value of $\Delta\Pi$ is the sum of the lysozyme, $\Delta\Pi_{\mathrm{L}}$, and salt contribution, $\Delta\Pi_{\mathrm{S}}$, to the total osmotic pressure. The variables $\Pi_{\mathrm{Lm}}$ and $\Pi_{\mathrm{Lp}}$

are the osmotic pressures of lysozyme at the fluid/membrane interface and in the permeate side, respectively. The variables $\Pi_{S0}$ and $\Pi_{Sp}$ are the osmotic pressures of NaCl in the feed solution and in the permeate side, respectively. The value of the osmotic pressure in the region adjacent to the membrane is considered equal to the one in the bulk of the solution ($\Pi_{S0}$). These osmotic pressures are given by

$$\Pi_L = \Re T\left[\frac{\rho\omega_L}{M_L} + B_{LL}(\rho\omega_L)^2\right] \tag{15a}$$

$$\Pi_S = 8.051 \times 10^7 \omega_S \text{ (Pa)} \tag{15b}$$

In these equations, $\Re$ is ideal gas constant, $T$ is the absolute temperature in Kelvin, $M_L$ is the lysozyme molecular weight and $B_{LL}$ is the second virial osmotic coefficient for lysozyme. The coefficient $B_{LL}$ is dependent on the NaCl concentration and a correlation for the variation of $B_{LL}$ with the NaCl mass fraction, $\omega_S$, is obtained by the fitting of Velev et al. [16] data (Eq. (16)). The units of $B_{LL}$ in Eq. (16) are mol/m$^3$/kg$^2$.

$$B_{LL} = \begin{cases} -5.60 \times 10^{-1} \cdot \omega_S + 3.25 \times 10^{-3} \\ \quad 0 \leqslant \omega_S \leqslant 0.0058 \\ -1.63 \times 10^{-2} \cdot \omega_S + 6.47 \times 10^{-5} \\ \quad 0.0058 < \omega_S \leqslant 0.029 \end{cases} \tag{16}$$

*Set II*—The salt concentration polarization neglected in set I is now being considered and the Eqs. (6) and (11b) are incorporated in the system of model equations. As well as in set I, cross diffusion is neglected. The Eqs. (5), (6), (11a) and (11b) are then simplified due to the vanishing of the cross diffusion terms. In Eq. (10), $\Delta\Pi$ is now given by the following equation:

$$\begin{aligned}\Delta\Pi &= \Delta\Pi_L + \Delta\Pi_S \\ &= (\Pi_{Lm} - \Pi_{Lp}) + (\Pi_{Sm} - \Pi_{Sp})\end{aligned} \tag{17}$$

One should remark that in contrast with Eq. (14), in Eq. (17) the osmotic pressure of NaCl at the fluid/membrane interface ($\Pi_{Sm}$) is different from the bulk feed solution value, $\Pi_{S0}$. In agreement with that, Eqs. (2)–(6) are solved together with Eqs. (7)–(11b) as boundary conditions.

*Set III*—Simulations incorporating salt concentration polarization (set II) and cross diffusion are now carried out. The Eqs. (2)–(6) are solved together with Eqs. (7)–(11b) without any simplification.

Table 2
Summary of the CFD simulations

| y (yes), n (no) | Set | | |
|---|---|---|---|
| | *I* | *II* | *III* |
| Incorporation of NaCl concentration polarization | *n* | *y* | *y* |
| Incorporation of cross diffusion | *n* | *n* | *y* |

Table 2 is a simplified descriptive summary of the different simulations sets.

## 7. Discussion of results

Simulations of the fluid flow and mass transfer phenomena occurring during the UF of water/ lysozyme/ NaCl solutions were performed. A simplified diagram describing the input/ output data is shown in Fig. 7.

The qualitative behaviour of the variation of the experimental fluxes with salt concentration, described in point 5.2 and displayed in Fig. 6(a), is well anticipated as there is a decrease of the effective pressure ($\Delta P_{effective} = \Delta P - \Delta\Pi$) when the osmotic pressure differences are taken into consideration. In fact, the CFD simulations based on Eqs. (2)–(11b), allow the prediction of the protein and salt concentration profiles developed from higher concentrations adjacent to the membrane to lower concentration values at the bulk of the feed solution. In particular, these solutes concentrations adjacent to the membrane yielded by CFD, are key parameters for the accurate osmotic pressure calculation.

As already described, three types of simulations corresponding to three different assumptions of mass transfer conditions were performed (simulation sets I, II and III). Fig. 8 displays the predicted permeation fluxes (averaged over the entire membrane length: $v_{p,av}$) and compares them with the experimental ones.

As it can be observed, all the simulations sets predict very well the permeation fluxes at lower pressures, till $4 \times 10^5$ Pa, for all solutions. The differences between predicted and experimental values increase with pressure and are larger at the higher pressures of $6 \times 10^5$ and $8 \times 10^5$ Pa. If the NaCl continuity equation is not incorporated in the simulations (set I), one concludes that these deviations are more pronounced for the higher values of NaCl concentration. If both lysozyme and NaCl continuity equations are taken into consideration as in set II of simulations, the predicted values are closer to the experimental ones, and that is more pronounced for salt concentrations of 0.1 and 0.5 M (Fig. 8(c) and (d)). For the set III of simulations considering the

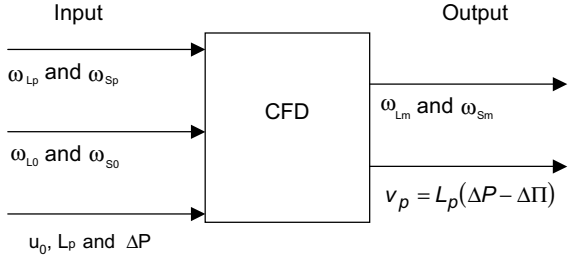


Fig. 7. Simulations input/output data.

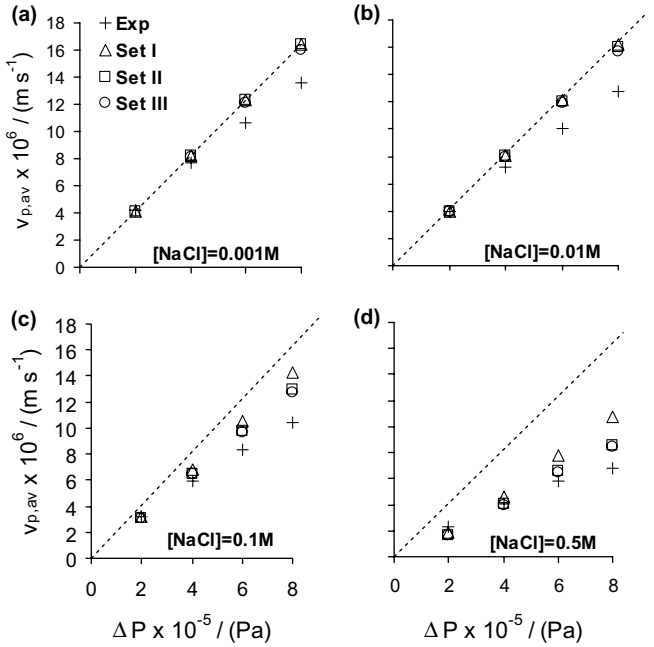


Fig. 8. Comparison between predicted and experimental permeation fluxes.

continuity equations for both solutes and cross diffusion effects, there is no significant improvement over the previous set II of simulations. There is clearly a closer agreement between experimental and predicted values for set II and III than that obtained for set I. It can then be stated that even for a UF membrane with a MWCO of 30 kDa and characterized by low values of NaCl rejection coefficients, the NaCl concentration polarization or the development of a NaCl concentration profile adjacent to the membrane, should be taken into account. It can also be concluded that for the present system membrane/ternary feed solution, cross diffusion has no significant effect in the permeation fluxes, and does not play any important role on the mass transport.

Regarding the important role of the salt concentration on the rejection coefficients to lysozyme and to NaCl, as described in point 5.2 and in relation to Fig. 6(b) and (c), one should discuss these results under the light of the electrical double layer theory. According to this theory, charged macromolecules can attract counter ions and that will affect the magnitude of its hydrodynamic radii. Lysozyme is a protein with the isoelectric (zero charge) point at pH ≅ 11. For pH values below the isoelectric point, the protein has an overall positive net charge. In this work, all solutions had pH values between 5.4 and 7.1. These values are far below the isoelectric point of lysozyme, hence the macromolecule has a strong positive net charge and an associated electrical double layer. In the electrical double layer, the electric potential decreases exponentially with a typical decay length called the *Debye length*, $\lambda_D$. For aqueous solutions of monovalent salts at 25 °C, the Debye length is given by Eq. (18)

$$\lambda_D\ (\text{nm}) = \frac{0.304}{\sqrt{C_{\text{salt}}}} \tag{18}$$

In Eq. (18), $C_{\text{salt}}$ is the concentration of salt in solution, in mol/L. The values of $\lambda_D$ for the electrical double layer around molecules of lysozyme, were calculated for the solutions used in the permeation experiments and are presented in Table 3. The values shown in Table 3 take into account the existence of protein stabilising salts, as already referred in point 5.2.

The sharp reduction of the Debye length shown in Table 3, is caused by the increase of the salt concentration in the solution and that reduces the hydrodynamic

Table 3
Calculation of the Debye lengths for the solutions of lysozyme ($C_{\text{commercial lysozyme}} = 0.3 - 0.35$ g/L) at different salt concentrations

| Solution of lysozyme | Debye length (nm) |
|---|---|
| no added salt | $11.8 < \lambda_D < 12.8$ |
| $C_{NaCl} = 0.001$ M | $7.46 < \lambda_D < 8.12$ |
| $C_{NaCl} = 0.01$ M | $2.94 < \lambda_D < 2.98$ |
| $C_{NaCl} = 0.1$ M | $\lambda_D = 0.96$ |
| $C_{NaCl} = 0.5$ M | $\lambda_D = 0.43$ |

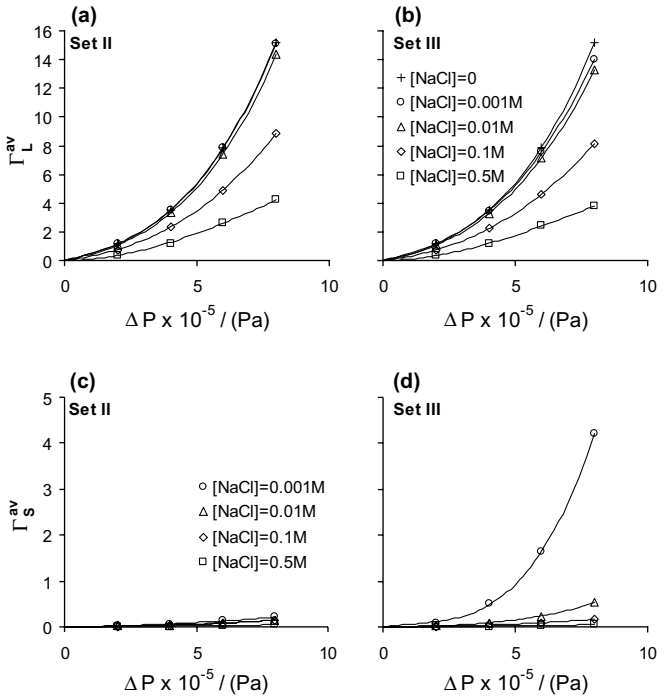


Fig. 9. Predicted values of the average concentration polarization of lysozyme and NaCl. Without cross diffusion (a,c) and with cross diffusion (b,d).

radii of the lysozyme molecules. Therefore, if one is considering that UF is mainly controlled by steric hindrance mechanisms, the decrease of the lysozyme rejection coefficient can be expected.

Fig. 9 presents the predicted values of the average concentration polarization coefficients ($\Gamma^{av}$) for both solutes, obtained from simulations II and III. The average concentration polarization coefficient for a solute A is given by $\Gamma_A^{av} = (\omega_{Am}^{av}/\omega_{A0}) - 1$, being $\omega_{Am}^{av}$ the value of $\omega_{Am}$ averaged over the entire membrane length. Comparing Fig. 9(a) with Fig. 9(b), one concludes that the phenomenon of cross diffusion has a marginal effect on the lysozyme concentration polarization. On the contrary, for the low NaCl concentrations of 0.001 and 0.01 M (Fig. 9(c) and (d)), cross diffusion plays a significant effect on the NaCl concentration polarization.

## 8. Conclusions

A UF membrane with a MWCO that should highly reject protein and let the salt permeate through presents experimental permeation characteristics that are dependent of the salt concentration, thus influencing the protein rejection:

- The increase of the salt concentration, produces a decrease on the lysozyme experimental rejection coefficient. Considering that UF is mainly controlled by steric hindrance mechanisms, such result can be qualitatively explained by the decrease of the lysozyme Debye length, i.e., the decrease of the protein hydrodynamic radius, induced by the increase on the concentration of the salt ions.

Moreover, the experimental results show the existence of important interactions between the solutes lysozyme and NaCl. Hence, the UF of the ternary system water/lysozyme/sodium chloride, requires a multicomponent mass transfer approach that can only be accurately carried out making recourse to CFD. In fact, the CFD local descriptions of the flow and mass transfer, allow the prediction of the salt and protein concentration polarization, making possible the following conclusions:

- The variation of the permeate fluxes with the salt concentration, is better predicted by CFD simulations incorporating the partial continuity equations for both protein and salt solutes.
- The effect of the cross diffusion on the protein concentration polarization is negligible.

- The effect of the cross diffusion on the salt concentration polarization is only important at very low salt concentrations.

## Acknowledgement

The authors acknowledge the financial support given by Fundação para a Ciência e Tecnologia (SFRH/BD/6149/2001).

## References

[1] R.F. Probstein, J.S. Shen, W.F. Leung, Ultrafiltration of macromolecular solutions at high polarization in laminar channel flow, Desalination 24 (1978) 1–10.
[2] A.L. Zydney, Stagnant film model for concentration polarization in membrane systems, J. Membr. Sci. 130 (1997) 275–281.
[3] P.L.T. Brian, Concentration polarization in reverse osmosis desalination with variable flux and incomplete salt rejection, Ind. Eng. Chem. Fundam. 4 (4) (1965) 439–445.
[4] T.K. Sherwood, P.L.T. Brian, R.E. Fisher, L. Dresner, Salt concentration at phase boundaries in desalination by reverse osmosis, Ind. Eng. Chem. Fundam. 4 (2) (1965) 113.
[5] V.M. Geraldes, V.A. Semião, M.N. de Pinho, Nanofiltration mass transfer at the entrance region of a slit laminar flow, Ind. Eng. Chem. Res. 37 (12) (1998) 4792–4800.
[6] V.M. Geraldes, V.A. Semião, M.N. de Pinho, The effect on mass transfer of momentum and concentration boundary layers at the entrance region of a slit with a nanofiltration membrane wall, Chem. Eng. Sci. 57 (5) (2002) 735–748.
[7] V.M. Geraldes, V.A. Semião, M.N. de Pinho, Nanofiltration modelling of mass transfer in slits with semi-permeable membrane walls, Eng. Comput.—Int. J. Comput. Aided Eng. Software 17 (2–3) (2000) 192–217.
[8] R.E. Lebrun, C.R. Bouchard, A.L. Rollin, T. Matsuura, S. Sourirajan, Computer simulation of membrane separation processes, Chem. Eng. Sci. 44 (2) (1989) 313.
[9] C.R. Bouchard, P.J. Carreau, T. Matsuura, S. Sourirajan, Modeling of ultrafiltration: predictions of concentration polarization effects, J. Membr. Sci. 97 (1994) 215.
[10] C. Rosén, C. Trägårdh, Computer simulations of mass transfer in the concentration boundary layer over ultrafiltration membranes, J. Membr. Sci. 85 (1993) 139.
[11] J.G. Albright, O. Annunziata, D.G. Miller, L. Paduano, A.J. Pearlstein, Precision measurements of binary and multicomponent diffusion coefficients in protein solutions relevant to crystal growth: Lysozyme chloride in water and aqueous NaCl at pH 4.5 and 25 °C, J. Am. Chem. Soc. 121 (1999) 3256–3266.
[12] O. Annunziata, L. Paduano, A.J. Pearlstein, D.G. Miller, J.G. Albright, Extraction of thermodynamic data from ternary diffusion coefficients. Use of precision diffusion measurements for aqueous lysozyme chloride—NaCl at 25 °C to determine the change of lysozyme chloride chemical potential with increasing NaCl concentration, J. Am. Chem. Soc. 122 (2000) 5916–5928.
[13] S. Patankar, Numerical Heat Transfer and Fluid Flow, McGraw-Hill, New York, 1982.
[14] B. Kunst, S. Sourirajan, An approach to the development of cellulose acetate ultrafiltration membranes, J. Appl. Polym. Sci. 18 (1974) 3423.
[15] G.L. Peterson, A simplification of the protein assay method of Lowry et al. which is more generally applicable, Anal. Biochem. 83 (1977) 346.
[16] O.D. Velev, E.W. Kaler, A.M. Lenhoff, Protein interactions in solution characterized by light and neutron scattering: comparison of lysozyme and chymotrypsinogen, Biophys. J. 75 (1988) 3211–3224.